Available online at www.sciencedirect.com

ScienceDirect

journal homepage: www.elsevier.com/locate/he

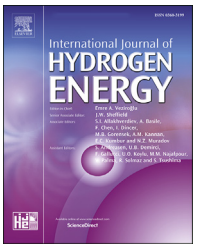

Aspen Plus model of an alkaline electrolysis system for hydrogen production

Mónica Sánchez [a,b,*], *Ernesto Amores* [a], *David Abad* [a], *Lourdes Rodríguez* [c], *Carmen Clemente-Jul* [b]

[a] *Centro Nacional del Hidrógeno (CNH2), Prolongación Fernando El Santo s/n, 13500, Puertollano, Ciudad Real, Spain*

[b] *Departamento de Energía y Combustibles, E.T.S.I de Minas y Energía, Universidad Politécnica de Madrid (UPM), C/ Ríos Rosas 21, 28003, Madrid, Spain*

[c] *Universidad Europea de Madrid (UEM), C/Tajo s/n, Urbanización El Bosque, 28670 Villaviciosa de Odón, Madrid, Spain*

HIGHLIGHTS

- A model of an alkaline electrolysis (AEL) plant has been developed using Aspen Plus.
- A custom cell stack model has been integrated in Aspen Plus as a subroutine.
- Simulations have been conducted to analyze the performance of an AEL plant.
- The proposed model constitutes a useful tool to carry out system optimization.

ARTICLE INFO

Article history:
Received 16 September 2019
Received in revised form
13 November 2019
Accepted 4 December 2019
Available online xxx

Keywords:
Hydrogen production
Alkaline water electrolysis
Balance of plant
System simulation
Aspen plus model
Process optimization

ABSTRACT

A model of an alkaline electrolysis plant is proposed in this paper, including both stack and balance of plant, with the objective of analyzing the performance of a complete electrolysis system. For this purpose, Aspen Plus has been used in this work due to its great potential and flexibility. Since this software does not include codes for modelling the electrolysis cells, a custom model for the stack has been integrated as a subroutine, using a tool called Aspen Custom Modeler. This stack model is based on semi-empirical equations which describe the voltage cell, Faraday efficiency and gas purity as a function of the current. The rest of the components in the electrolysis plant have been modelled with standard operation units included in Aspen Plus. Simulations have been carried out in order to evaluate and optimize the balance of the plant of an alkaline electrolysis system for hydrogen production. Also, a parametric study has been conducted. The results show that increasing the operation temperature and reducing the pressure can improve the overall performance of the system. The proposed model in this work for the alkaline electrolyzer can be used in the future to develop a useful tool to carry out techno-economic studies of alkaline electrolysis systems integrated with other process.

* *Corresponding author*. Centro Nacional del Hidrógeno (CNH2), Prolongación Fernando El Santo s/n, 13500 Puertollano, Ciudad Real, Spain.

E-mail addresses: monica.sanchez@cnh2.es (M. Sánchez), ernesto.amores@cnh2.es (E. Amores), david.abad@cnh2.es (D. Abad), marialourdes.rodriguez@universidadeuropea.es (L. Rodríguez), carmen.clemente@upm.es (C. Clemente-Jul).

https://doi.org/10.1016/j.ijhydene.2019.12.027

Abbreviations, nomenclature and units

Acronyms

ACM	Aspen custom modeler
AEL	Alkaline electrolysis
BoP	Balance of plant
CAPEX	Capital expenditure
HTO	Hydrogen-to-oxygen
LHV	Low heating value
NRTL	Non-Random Two-Liquid
OTH	Oxygen-to-hydrogen
RES	Renewable energy sources
RMS	Root mean square

Symbols

A	Area, m^2
C	Parameter related to gas purity (temperature)
d	Parameter related to ohmic resistance (pressure)
E	Parameter related to gas purity (pressure)
f	Parameter related to Faraday efficiency
F	Faraday constant, 96485 C mol^{-1}
G	Gibbs energy, J mol^{-1}
H	Enthalpy, J mol^{-1}
i	Current density, A m^{-2}
I	Current, A
n	Molar flow rate, mol s^{-1}
N	Number of cells of the stack
p	Pressure, bar
Q	Thermal power or heat transfer, W
r	Parameter related to ohmic resistance (temperature)
s	Coefficient for overvoltage on electrodes, V
S	Entropy, J mol^{-1} $°C^{-1}$
t	Coefficient for overvoltage on electrodes
T	Temperature, °C
V	Voltage, V
W	Electric power, W
z	Electrons transferred per ion
η	Efficiency, %
$\hat{\eta}$	Overpotential, V

Subscripts

an	Anode
cat	Cathode
cell	Alkaline water electrolysis cell
conc	Concentration
en	Energy
excess	Excess or waste
exp	Experimental
F	Faraday
gen	Generate or produced
lcoss	Loss (via heat radiation)
NET	Overall or net
ohm	Ohmic
prod	Production
rev	Reversible
stack	Alkaline water electrolysis stack
th	Theoretical or model
tn	Thermoneutral

Introduction

Renewable energies have had a spectacular development in recent years. However, a massive penetration of renewable energy sources (RES) can affect adversely to the grid stability due to its variability and unpredictability [1]. In this context, hydrogen could play a key role as large-scale energy storage, through the water electrolysis [2].

Currently, alkaline water electrolysis (AEL) is the most mature electrolysis technology and it is commercially available for large-scale hydrogen production. Typical alkaline electrolysis cell consists in two Ni-based electrodes immersed in a liquid electrolyte (usually a 30–35 wt% aqueous KOH solution) separated by a porous diaphragm. The operating temperature is between 60 and 90 °C and the pressure is commonly below 30 bar. The purity of the hydrogen produced is in the range of 99.5–99.9%, which can be increased up to 99.999% by catalytic gas purification systems [3]. Therefore, the key to this technology is its availability and the low specific cost compared to other electrolysis technologies [4].

However, the alkaline water electrolysis still presents certain limitations related to the low current density and the influence of the dynamic operation on the gas purity, efficiency and durability [2–5]. R&D efforts are carried out in order to improve the performance of alkaline electrolysis technology, mainly focus on:

- Development of advanced electrocatalysts to decrease the electrode overvoltage [6–9].
- Minimization of the space between the electrodes to reduce the ohmic losses and can operate at higher current densities [10,11].
- Development of new exchange inorganic membranes to replace the liquid electrolyte. The use of these membranes allows to reduce the crossover produced trough current porous diaphragms [10,12–14].

On the other hand, modelling is an important tool for the design and optimization of electrolysis systems [15]. Most of alkaline electrolysis models are focused on describing the electrochemical behavior of cell/stack. Generally, it consists in a mathematical description of the polarization curve and Faraday efficiency by analytical models [16,17] or empirical models [18–23]. In addition, thermal models are developed and integrated with electrochemical models in order to take into account the influence of the temperature [16,18,21,23]. However, only a few works consider the electrolysis system

Please cite this article as: Sánchez M et al., Aspen Plus model of an alkaline electrolysis system for hydrogen production, International Journal of Hydrogen Energy, https://doi.org/10.1016/j.ijhydene.2019.12.027

[20,24–27] and none of the models found in the literature describes the performance of a whole electrolysis plant including all the components [15].

The design and configuration of the balance of plant (BoP) and auxiliary systems have a high influence on the performance of the electrolysis cells, as well as, cost, efficiency and lifetime. The balance of plant represents approximately 30% of the capital cost (CAPEX) in an alkaline electrolyzer and the stack efficiency can be considerably reduced if the design of the auxiliary systems is not optimized [4,25,28]. Thus, the development of models including all components of the plant is necessary to optimize alkaline electrolysis systems powered by renewable energy sources, identify technical improvements related to auxiliary systems and reduce its consumption during part-load operation.

In this work, a steady state model of an alkaline electrolysis plant is proposed considering both alkaline water electrolysis cell stack and system. The system includes all the components of the balance of the plant such as deionised water supply, gas-liquid separator vessels, heat exchangers, pumps and the cooling loop. Due to the difficulty of implementing mathematical model at a system level in a flexible way, Aspen Plus software has been used in this work. Aspen Plus is one of the most widely used software in the industry for process modelling, equipment design and system optimization. The software is based on a modular operation and multi-flowsheet architecture enabling the development of easily adaptable models. Also, it contains libraries of chemicals and predetermined unit operation models that simplify greatly the design process [29].

However, Aspen Plus or Aspen HYSYS do not include codes for modelling the electrochemical cells, so there are only a few electrolysis models developed using this type of software [30–33]. Typically, these works are based on modelling the electrolysis cell using standard components available in the software. However, this approach is not able to describe appropriately the electrochemical process. So, novel models are required to describe in Aspen Plus the specific electrochemical phenomena that occur during water electrolysis.

In fact, the novelty of the present study lies here: a semi-empirical model for describing the performance of the cell/stack developed in a previous work [34] has been integrated in Aspen Plus as a subroutine, using a tool called Aspen Custom Modeler (ACM). This custom electrolysis model is able to predict in an accurate way, the cell stack voltage, the hydrogen and oxygen production and the quantity of hydrogen in the oxygen (HTO) due to the crossover in function of temperature, pressure and current density. The rest of the components in the electrolysis plant have been modelled with standard operation units included in Aspen Plus.

So, the integration of this customized model with the rest of the components of the balance of plant allows having a complete and innovative model of an alkaline electrolysis plant. The proposed model constitutes a useful tool to carry out system level optimization in order to maximize the overall efficiency. Using this mathematical tool, simulations have been carried out to obtain mass and energy balances of each subcomponent and the entire system. The results allow to analyze the thermodynamic system behavior and optimize the overall efficiency. Also, since the model developed is applicable for a wide operating range, a parametric study has been conducted, in order to investigate the influence of temperature, pressure and current density on the global performance of the alkaline electrolysis plant.

Therefore, this Aspen Plus model could be used as an intermediate tool to evaluate alkaline electrolysis plants linked to renewable energy sources, since the model is able to predict the performance of the stack and auxiliary systems at different loads (power input) in steady operation conditions. In order to evaluate the operation of the complete system during the transient periods, a dynamic model could be built from this using Aspen Dynamics in next steps.

Aspen Plus model

The model of an alkaline water electrolysis system has been developed using Aspen Plus [35], including alkaline electrolysis cell stack and the balance of plant (BoP). The simulation diagram of the AEL plant studied is shown in Fig. 1.

The cell stack (STACK) is the heart of the system. Electricity and heat are supplied to the cells to carry out the decomposition of water into hydrogen and oxygen through an electrochemical reaction shown in Eq. (1):

$$H_2O \rightarrow H_2 + \frac{1}{2}O_2 \quad (1)$$

Hydrogen (H2-STACK) and oxygen (O2-STACK) produced in cell stack are led with the electrolyte (KOH, 35%wt) to the liquid-gas separation vessels (SEP-H2 and SEP-O2, respectively), where the electrolyte is separated from the gas and returned back to the stack by recirculation pumps (PUMP-R1 for cathode circuit and PUMP-R2 for anode circuit). Both KOH recycles (R–H2-KOH and R–O2-KOH) pass through a heat exchanger (IC-R1 and IC-R2, respectively) to cool down the electrolyte before entering the stack (R-INLET). The cooling circuit is composed by an air-cooler (FAN) and a cooling pump (PUMP-COOL) which directs the cooling water (COOL-IN) through the heat exchangers integrated in the electrolyte recirculation loops to remove the waste heat and maintain the temperature in the cells.

The hydrogen and oxygen separated in the biphasic separation vessels pass through water traps (TRAP-H2 and TRAP-O2 respectively) to eliminate the maximum amount of condensate water. Finally, deionised water with conductivity of 5 μS/cm (H2O-IN) is fed from a water tank into the oxygen separator (SEP-O2) by a pump (PUMP-H2O) to provide water to electrolysis process (H2O-FEED).

Alkaline water electrolysis stack operation unit

Since Aspen Plus does not include an operation unit for modelling an alkaline electrolysis cell stack, in the present study, an alkaline water electrolysis stack model has been integrated in Aspen Plus as a subroutine, using Aspen Custom Modeler (ACM). This tool allows to create a custom operation unit, so the cell stack model is incorporated into the overall process to continue with the system simulation [36]. To develop this, firstly an Aspen Properties file must be created and imported to Aspen Custom Modeler tool in order to define

Please cite this article as: Sánchez M et al., Aspen Plus model of an alkaline electrolysis system for hydrogen production, International Journal of Hydrogen Energy, https://doi.org/10.1016/j.ijhydene.2019.12.027

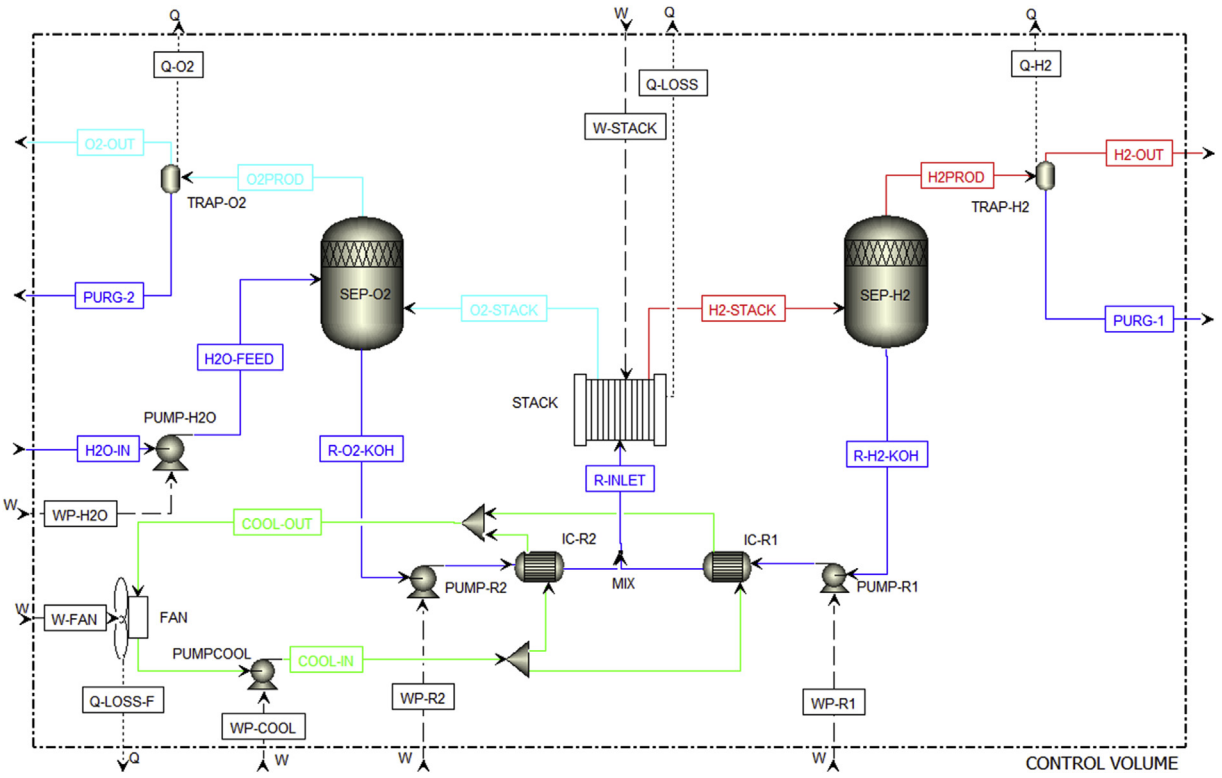

Fig. 1 – Aspen Plus process flow diagram of an alkaline electrolysis plant.

the components and choose the property method which will be used. In this case, a NRTL (Non-Random Two-Liquid) model has been used to carry out the simulations. The different equations, parameters and variables are written in the ACM reference language, assuring zero degrees of freedom and defining the input/output parameters.

For the stack operation unit developed in Aspen Custom Modeler (see Fig. 2), the electrochemical model for the alkaline electrolysis cells and all the equations related to the mass and energy balances that take place in the stack have been included. The necessary inputs to carry out simulations will be the electric power input, number of cells, active area of the electrode, stack temperature and operation pressure.

In addition, the ACM tool allows to build a personalized icon and connect the different material, heat or work streams. Once completed this, ACM simulates the model to verify its performance and export it to the Aspen Plus Library where is incorporated into the palette to be used as the rest of the Aspen Plus standard operation units.

Electrochemical model

The electrochemical model for the alkaline electrolysis cells has been developed in a previous work [34]. This model is able to predict the electrochemical behavior of an alkaline water electrolysis stack under different operating conditions, such as, temperature (T) and pressure (p). The proposed equations allow determining polarization curve, Faraday efficiency and gas purity, as a function of the current, basing on both physical principles related to the electrolysis process and statistical data [34,37–39].

The polarization curve analyzes the different overpotentials that occur during the electrolysis of water in order to determine the cell potential (V_{cell}) according to the current density. For the reaction to occur, a minimum voltage is required, which is known as reversible voltage (V_{rev}), corresponding to 1.23 V at standard conditions (1 bar and 25 °C) [37]. However, the cell voltage (V_{cell}) is always higher than theoretical one by the appearance of a series of overpotentials due to kinetic and resistive effects [23,37,38]. So, the real cell

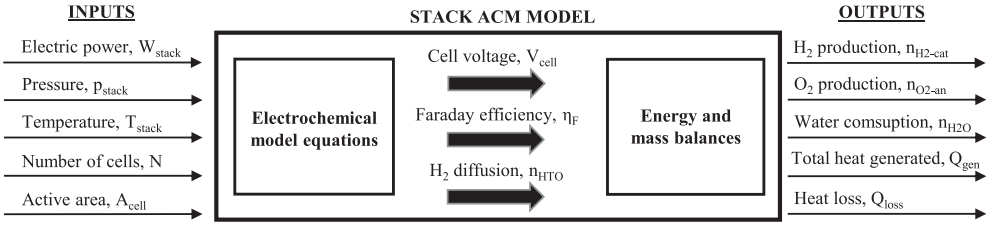

Fig. 2 – Operation unit developed in Aspen Custom Modeler for modelling the stack.

Please cite this article as: Sánchez M et al., Aspen Plus model of an alkaline electrolysis system for hydrogen production, International Journal of Hydrogen Energy, https://doi.org/10.1016/j.ijhydene.2019.12.027

voltage (V_{cell}) can be defined as the sum of reversible voltage and each of these overpotentials ($\hat{\eta}$), activation overvoltages ($\hat{\eta}_{cat}$, $\hat{\eta}_{an}$), ohmic overpotentials ($\hat{\eta}_{ohm}$) and concentration overpotentials ($\hat{\eta}_{conc}$) [23,37,38], as shown in Eq. (2).

$$V_{cell} = V_{rev} + (\hat{\eta}_{cat} + \hat{\eta}_{an} + \hat{\eta}_{ohm} + \hat{\eta}_{conc}) \quad (2)$$

The polarization curve can be determined using a semi-empirical model. In this regard, one of the most widely used models to describe the electrochemical response of an electrolyzer was proposed by Ulleberg [18] in 2003. So, taking as reference this model, a more comprehensive equation has been developed (Eq. (3)) in a previous work [34], including additional parameters and new empirical relationships to model temperature (T), pressure (p) and current density (i). Regarding the concentration overpotentials, these occur at very high current densities, above from the usual range of operation of an electrolyzer, so they have not been considered in Eq. (3).

$$V_{cell} = V_{rev} + [(r_1 + d_1) + r_2 \cdot T + d_2 \cdot p]i + s \cdot \log\left[\left(t_1 + \frac{t_2}{T} + \frac{t_3}{T^2}\right)i + 1\right] \quad (3)$$

On the other hand, it is possible to measure the effectiveness of the process using the Faraday efficiency (η_F), by comparing the moles produced ($n_{H2,\ prod}$) and the theoretical moles that should be produced during the same time ($n_{H2,\ th}$) [38]. This parameter is defined in Eq. (4):

$$\eta_F = \frac{n_{H2,prod}}{n_{H2,th}} \quad (4)$$

In a similar way to the polarization curve, the Faraday's efficiency can be also modelled by an empirical expression for a given temperature using 4 parameters for this purpose such as Eq. (5) [18,34]. The pressure has not been included due to its slight influence:

$$\eta_F = \left(\frac{i^2}{f_{11} + f_{12} \cdot T + i^2}\right) \cdot (f_{21} + f_{22} \cdot T) \quad (5)$$

Finally, a model for the diffusion of hydrogen to oxygen (HTO) has been proposed in Eq. (6) based on the results obtained in previous works [19,34], considering the influence of temperature and pressure on the purity of the gases:

$$HTO = \left[C_1 + C_2 \cdot T + C_3 \cdot T^2 + (C_4 + C_5 \cdot T + C_6 \cdot T^2) \cdot exp\left(\frac{C_7 + C_8 \cdot T + C_9 \cdot T^2}{i}\right) \times\right] + \left[E_1 + E_2 \cdot p + E_3 \cdot p^2 + (E_4 + E_5 \cdot p + E_6 \cdot p^2) \cdot exp\left(\frac{E_7 + E_8 \cdot p + E_9 \cdot p^2}{i}\right)\right] \quad (6)$$

All coefficients and parameters of the model have been calculated by means of a non-linear regression using MATLAB, taking as input experimental data obtained previously [23,34]. Table 1 shows the values used in this paper [34].

Mass balances

The hydrogen production rate at the cathode depends on the electrochemical behavior of the cells and can be determined using the Faraday efficiency by Eq. (7) [40]:

$$n_{H_2,prod} = \eta_F \cdot \frac{I}{z \cdot F} \cdot N \quad (7)$$

Table 1 – Coefficients considered for the electrochemical model of an alkaline water electrolysis cell [34].

Model	Coefficient	Value	Unit
Polarization curve	r_1	4.45153×10^{-5}	$\Omega\ m^2$
	r_2	6.88874×10^{-9}	$\Omega\ m^2\ ^\circ C^{-1}$
	d_1	-3.12996×10^{-6}	$\Omega\ m^2$
	d_2	4.47137×10^{-7}	$\Omega\ m^2\ bar^{-1}$
	s	0.33824	V
	t_1	−0.01539	$m^2\ A^{-1}$
	t_2	2.00181	$m^2\ ^\circ C\ A^{-1}$
	t_3	15.24178	$m^2\ ^\circ C^2\ A^{-1}$
Faraday efficiency	f_{11}	478645.74	$A^2\ m^{-4}$
	f_{12}	−2953.15	$A^2\ m^{-4}\ ^\circ C^{-1}$
	f_{21}	1.03960	–
	f_{22}	−0.00104	$^\circ C^{-1}$
Gas purity (hydrogen in oxygen)	C_1	0.09901	–
	C_2	−0.00207	$^\circ C^{-1}$
	C_3	1.31064×10^{-5}	$^\circ C^{-2}$
	C_4	−0.08483	–
	C_5	0.00179	$^\circ C^{-1}$
	C_6	-1.13390×10^{-5}	$^\circ C^{-2}$
	C_7	1481.45	$A\ m^{-2}$
	C_8	−23.60345	$A\ m^{-2}\ ^\circ C^{-1}$
	C_9	−0.25774	$A\ m^{-2}\ ^\circ C^{-2}$
	E_1	3.71417	–
	E_2	−0.93063	bar^{-1}
	E_3	0.05817	bar^{-2}
	E_4	−3.72068	–
	E_5	0.93219	bar^{-1}
	E_6	−0.05826	bar^{-2}
	E_7	−18.38215	$A\ m^{-2}$
	E_8	5.87316	$A\ m^{-2}\ bar^{-1}$
	E_9	−0.46425	$A\ m^{-2}\ bar^{-2}$

The production of oxygen (Eq. (10)) and consumption of water (Eq. (11)) are determined according to the reaction stoichiometry (Eq. (1)). Due to its importance, the mass balance takes into account the amount of hydrogen that is diffused across the diaphragms (Eq. (9)). On the other hand, since the diffusion of oxygen to hydrogen (OTH) is approximately 0.1–0.5% [41], has been considered negligible. Therefore, the mass balance for each component is expressed as:

$$n_{H_2,cat} = n_{H_2,prod} \quad (8)$$

$$n_{H_2,an} = n_{HTO} \quad (9)$$

$$n_{O_2,an} = n_{O_2,prod} = \frac{1}{2}\ n_{H_2,prod} \quad (10)$$

$$n_{H_2O} = n_{H_2,prod} \quad (11)$$

The gases produced, hydrogen and oxygen, leave the stack immersed in a KOH electrolyte flow, which is latter separated and recirculated to the stack.

Energy balances

The total energy demand for electrolytic hydrogen production is given by the enthalpy of reaction (ΔH), according to Eq. (12) [3]:

$$\Delta H = \Delta G + T\Delta S \quad (12)$$

Please cite this article as: Sánchez M et al., Aspen Plus model of an alkaline electrolysis system for hydrogen production, International Journal of Hydrogen Energy, https://doi.org/10.1016/j.ijhydene.2019.12.027

When all the energy needed for the electrochemical process is provided of electricity, the minimum voltage to carry out water electrolysis in adiabatic conditions, is the thermoneutral cell voltage (V_{tn}) [6], according to Eq. (13):

$$V_{tn} = \frac{\Delta H}{z \cdot F} \tag{13}$$

Thus, if cell potential is higher than thermoneutral voltage, no external heat is needed for carrying out the electrochemical reaction. On the contrary, a heat is generated in the process directly proportional to the difference between the cell voltage and the thermoneutral voltage [42], according to Eq. (14). A part of this heat generated is assumed to be lost via heat radiation from the electrolysis cells (Q_{loss}), thus, the net excess heat is given by Eq. (15):

$$Q_{gen} = N \cdot I \cdot (V_{cell} - V_{tn}) \tag{14}$$

$$Q_{excess} = Q_{gen} - Q_{loss} \tag{15}$$

The excess heat results in an increase of the temperature of electrolyte flow and gases produced in the stack. For this reason, it must be continuously removed in order to ensure a constant operating temperature.

Balance of plant

The balance of plant includes all the equipment needed to operate the stack, such as, deionised water supply, heat exchangers, gas-liquid separator vessels, circulation pumps and the cooling loop. As it can be seen in Fig. 1, the process flow model has been developed to include all the major components that would be present in an actual alkaline electrolysis plant.

Most components in the balance of the plant have been modelled using the standard elements found in Aspen Plus software. Introducing system boundary conditions, individual component efficiencies and operating parameters to the process, the Aspen software performs energy and mass balances across all components to predict fluid conditions around the system including thermodynamic data for all chemical species involved in the process [35].

System efficiency

To assess the overall performance of the system, the energy efficiency should be calculated. The energy efficiency represents the ratio of the energy contained in the useful products of a process to the energy contained in all input streams [43]. Therefore, the energy efficiency for hydrogen production from an electrolysis system is formulated as follows (Eq. (16)) [42]:

$$\eta_{en} = \frac{n_{H2,OUT} \cdot LHV_{H2}}{W_{NET}} \tag{16}$$

where LHV_{H2} is the hydrogen lower heating value; $n_{H2,\ OUT}$ is the outlet flow rate of hydrogen in the electrolysis plant; W_{NET} is the electric power input to the AEL system. For the complete alkaline electrolysis system shown in Fig. 2, the net power is defined by Eq. (17):

$$W_{NET} = W_{stack} + W_{pump-R1} + W_{pump-R2} + W_{pump-H2O} + W_{pump-COOL} + W_{fan} \tag{17}$$

where $W_{pump\text{-}R1}$, $W_{pump\text{-}R2}$, $W_{pump\text{-}H2O}$, $W_{pump\text{-}cool}$ and W_{fan} denotes power input to the pumps of the system and fan consumption, respectively. W_{stack} is the electric power input for the stack operation and can be determined according to Eq (18), where N is the number of cells of stack:

$$W_{stack} = V_{stack} \cdot I = (V_{cell} \cdot N) \cdot (i \cdot A_{cell}) \tag{18}$$

Results and discussion

As already discussed, to carry out the simulation in Aspen Plus, the data required are introduced in the developed model in order to calculate the different outputs. Table 2 lists the input for the alkaline electrolysis plant simulation at base-case conditions.

Also, the following assumptions are considered to simplify the simulation process:

- All processes operate at steady state
- All the gases in the system behave like ideal gases
- 10% of the total heat produced by the stack is lost due to convection and radiation
- Liquid deionised H_2O is fed to the system in a reference environment condition at 298 K
- The hydrogen and oxygen output are at 298 K
- The electrolyte recirculation is fixed at 15 l min^{-1}
- AEL stack is operated at balanced anode and cathode pressure

Experimental model validation

For carrying out the experimental tests and the validation of the model, a cell stack composed of 12 bipolar alkaline electrolysis cells of 1000 cm^2 surface area connected electrically in series, has been characterized at different operating conditions into a fully automated test bench developed by *Centro Nacional del Hidrógeno* (CNH2).

This test bench (Fig. 3), which has been described in detailed in previously published papers [34,44–46], has a capacity of 2.5 $Nm^3\ h^{-1}$ of hydrogen production and has been designed to be able to operate in a wide range of temperatures

Table 2 – Input data for the system simulation at base-case operation conditions (75 °C and 7 bar).

Parameter	Value	Unit
Stack working temperature, T_{stack}	75	°C
Operating system pressure, p_{stack}	7	bar
Electrolyte concentration	35	wt% KOH
Active electrode area, A_{cell}	1000	cm^2
Cell number, N	12	cells
Input power stack, W_{stack}	10	kW

Please cite this article as: Sánchez M et al., Aspen Plus model of an alkaline electrolysis system for hydrogen production, International Journal of Hydrogen Energy, https://doi.org/10.1016/j.ijhydene.2019.12.027

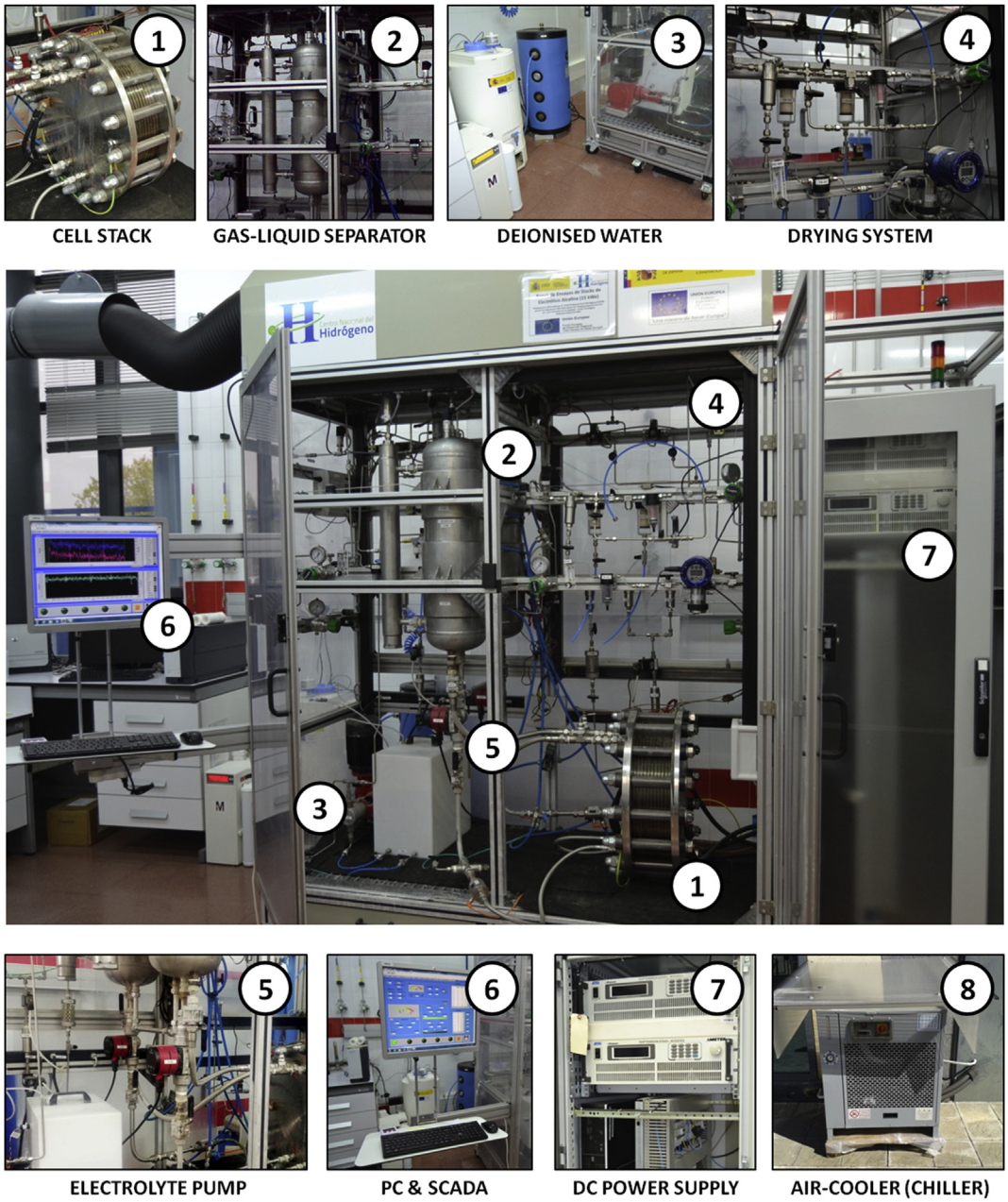

Fig. 3 – 15 kW alkaline water electrolysis test-bench developed by CNH2 [46].

(40–80 °C) and pressures (1–10 bar). Two programmable DC switching power supplies provide electrical power to the cells, with the possibility of being connected in series or parallel, reaching a maximum power of 15 kW (0–120 V and 0–500 A). The purity of the gases produced is monitored by on-line gas analyzers. An accurate thermal mass flow meter has been installed at the hydrogen output for measuring hydrogen production. Also, water flow rate of the cooling system for the electrolyzer is logged and collected. For thermal characterization, thermocouples are included in all the main streams of the system. The plant control unit is based on a PLC (programmable logic controller) that controls the system through a series of strategies optimized and acquires all the information provided by the different sensors.

The experimental data obtained in this test bench (potential, hydrogen production and gas purity) have been used to calculate the coefficients shown in Table 1, as previously mentioned [34]. Subsequently, simulated and measured values have been compared to ensure the accuracy and validity of the proposed model using the root-mean-square (RMS) error. Fig. 4 shows a parity chart of the model and experimental results used in this paper. The results show an excellent correlation between experimental and modelled data: the RMS error is approximately 5 mV per cell and lower than 1% for the Faraday efficiency and HTO [34]. This demonstrates the usefulness of the model to predict the electrolyzer response in other experimental conditions.

Please cite this article as: Sánchez M et al., Aspen Plus model of an alkaline electrolysis system for hydrogen production, International Journal of Hydrogen Energy, https://doi.org/10.1016/j.ijhydene.2019.12.027

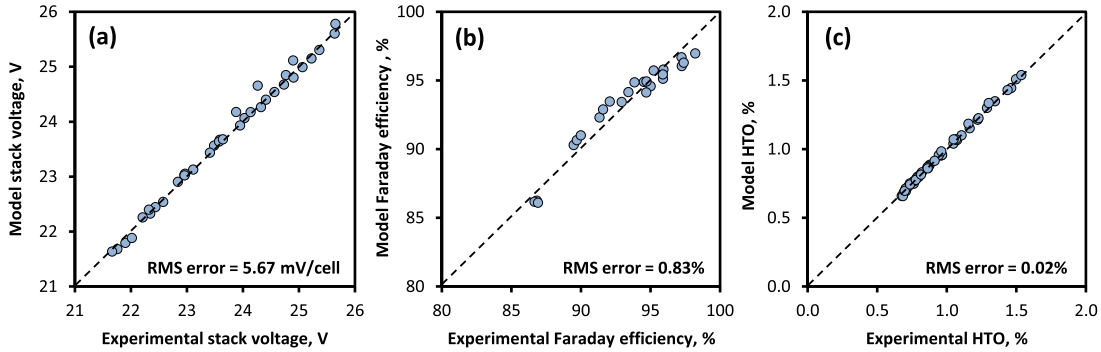

Fig. 4 – Parity chart of the model and experimental results: a) Stack voltage; b) Faraday efficiency; c) Gas purity.

Alkaline water electrolysis cell stack performance

In this section, a study has been conducted using the Aspen Plus model developed in this work to investigate the effect of operating temperature, pressure and current density on the performance of the cell stack. In the figures, all other parameters are fixed at base-case conditions (see Table 2). With this objective, it has been evaluated the polarization curve, overpotentials in the cell, power required by the stack, heat generated and required and the hydrogen crossover (*HTO*), among others.

Influence of the temperature and current density

Fig. 5a shows the polarization curve and power required by the alkaline electrolysis stack at different temperatures. According to the model, when the temperature increases from 50 °C to 80 °C, the voltage progressively reduces. As a consequence, the stack power required in the electrolysis decreases when the temperature is higher.

In Fig. 5b, the ohmic and activation overpotentials are showed individually. The ohmic overpotentials are related with the electrical resistance of the different materials of the electrolysis cell and the interfaces between them; while the activation overpotentials are as a consequence of the activation energy of reactions that occur on the electrodes. When the current density increases both overpotentials grow significantly, so that the overall potential is increased. As it can be seen the activation overpotentials dominate the voltage losses [47]. When the temperature increases, the activation overpotentials are reduced because the electrochemical reaction is faster [47]. On the other hand, the high conductivity of the electrolyte (KOH 35%) and stack design lead to a lower ohmic overpotential [48].

In order to analyze the heat requirements for the AEL stack operation is important to evaluate the heat production by the irreversibilities. As it can be seen in Fig. 5c, the heat production (due mainly to activation overpotentials) increases significatively with the current density and is lower at higher

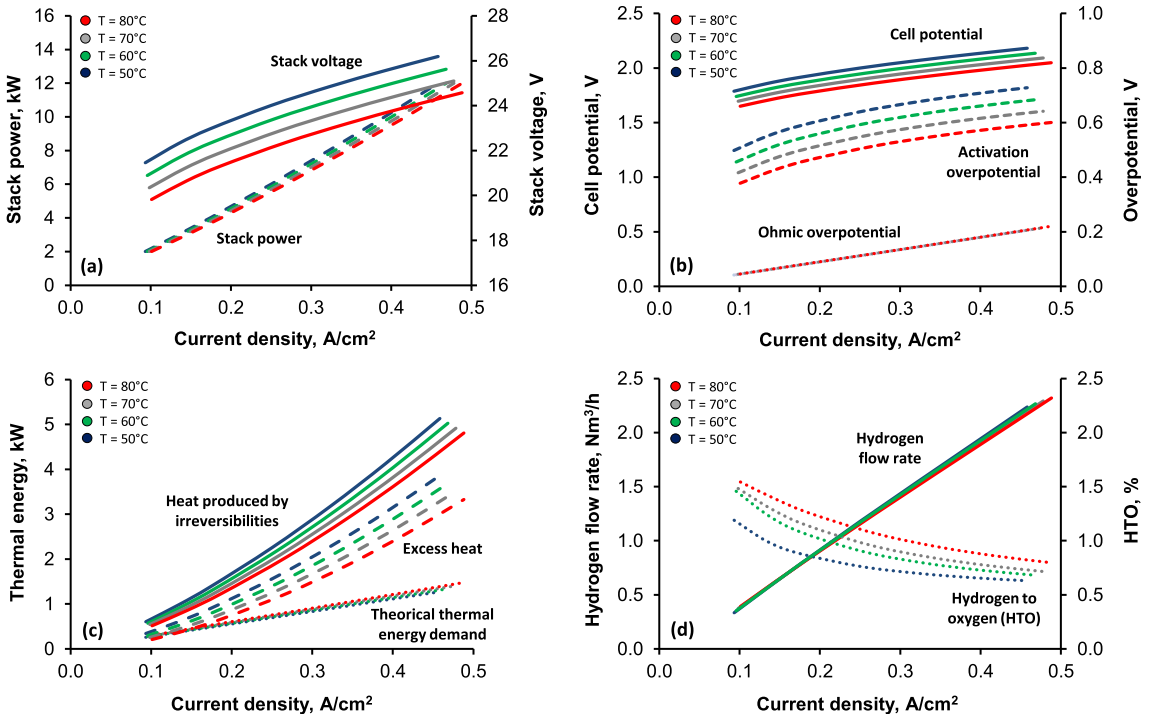

Fig. 5 – Effect of temperature on an AEL stack performance at 7 bar: a) Polarization curve and stack power required; b) Cell voltage and overpotentials; c) Heat generated, heat required and excess heat; d) Hydrogen flow rate and hydrogen crossover (*HTO*).

Please cite this article as: Sánchez M et al., Aspen Plus model of an alkaline electrolysis system for hydrogen production, International Journal of Hydrogen Energy, https://doi.org/10.1016/j.ijhydene.2019.12.027

temperature. For a better understanding, the theoretical thermal energy demand ($T\Delta S$) is also shown in the figure for comparison. It is observed that, in all the range studied, the heat production by overpotentials exceeds the energy required by the electrolysis process in adiabatic conditions. It means that, in this case, no external heat input is needed and the excess heat must be cooled in order to maintain the operation temperature constant.

Fig. 5d shows the hydrogen production and the content of hydrogen in oxygen (*HTO*) at different temperatures. The hydrogen production increases when the temperature is reduced. This is because an increase in temperature leads to a lower resistance, more parasitic current losses and so lower Faraday efficiencies [18]. Regarding to the content of hydrogen in oxygen (*HTO*), the results show that high temperatures have a great influence on the generated impurities, since the diffusion phenomena and the gas migrations increase significantly. On the other hand, as can be seen in Fig. 5d, at low current densities, the purity of the gases produced is significantly reduced. This is due to that the mentioned phenomena are mostly independent of the electrolyzer load, so when the production gas rate is low the percentage of total impurities is higher [34,39]. Thus, for safety reasons, the minimum applied current density in the tests was 0.1 A cm^{-2}.

Influence of the pressure and current density

Fig. 6a shows the polarization curve and power required by the alkaline electrolysis stack at different pressures. The main variation occurs in the ohmic overpotentials (Fig. 6b) due to a series of phenomena mainly related to the size of the gas bubbles generated during the electrolysis [34,49,50].

On the one hand, when the pressure raises the void fraction between electrodes is reduced due to smaller size of generated gas bubbles. This reduction in bubbles sizes also affects the effective contact area between electrodes and electrolyte, which results in lower ohmic resistance and required cell voltage [51]. On the other hand, the reversible cell voltage increases with the pressure. As a consequence, in the pressure range studied, these phenomena are counterbalanced and ohmic overpotentials increase slightly when the pressure increases. Regarding the activation overpotentials, the pressure has practically no perceptible influence.

In Fig. 6c is illustrated the heat generated, heat required and excess heat at different pressures. As shown, the heat production by irreversibilities increases at low pressures because although the stack voltage increases slightly from 5 to 9 bar, as discussed previously, the theoretical thermal energy demand ($T\Delta S$) is reduced at higher pressures. As with temperature (Fig. 5c), the heat production by overpotentials exceeds the energy required by the electrolysis process in adiabatic conditions for any pressure. As consequence, the excess heat must be removed to maintain the temperature in the cells.

Regarding to the content of hydrogen in oxygen (HTO), as can be seen in Fig. 6d, it increases strongly with decreasing the current density for all pressures. In addition, the results show that a higher pressure increases the impurities. This occurs because the pressure has a strong influence both on the solubility of the gases in the electrolyte and on the gas diffusion between the cathode and the anode inside the cell. About hydrogen flow rate, the effect of the pressure can be considered negligible.

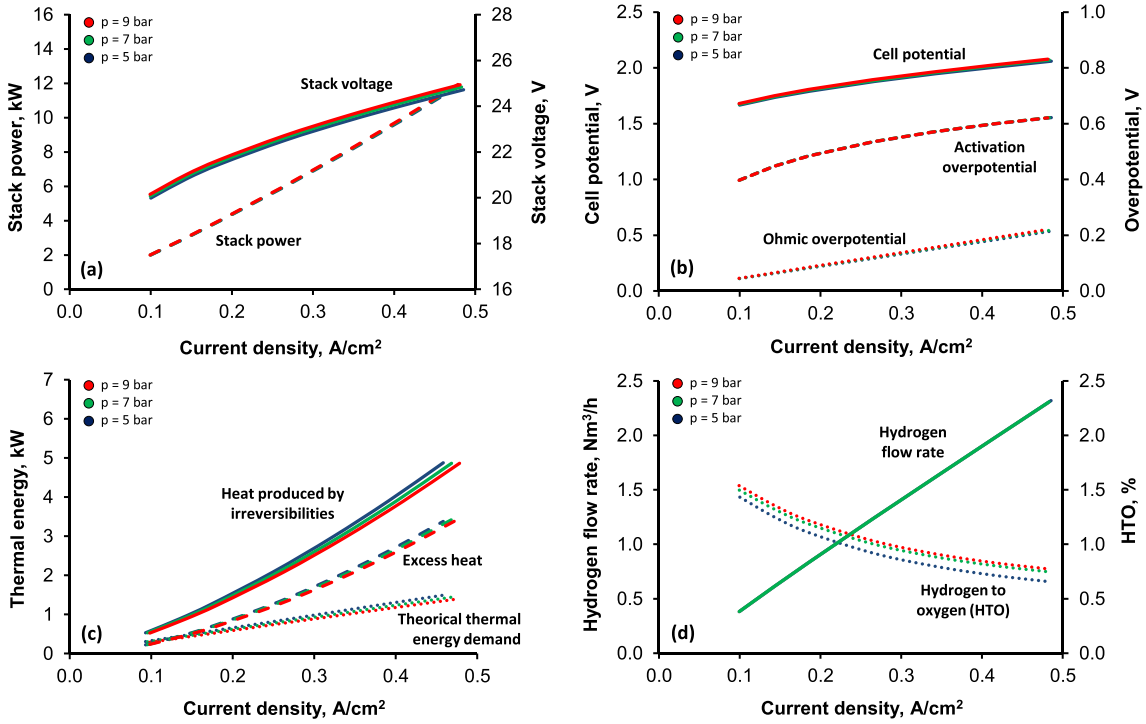

Fig. 6 – Effect of pressure on an AEL stack performance at 75 °C: a) Polarization curve and stack power required; b) Cell voltage and overpotentials; c) Heat generated, heat required and excess heat; d) Hydrogen flow rate and hydrogen crossover (*HTO*).

Please cite this article as: Sánchez M et al., Aspen Plus model of an alkaline electrolysis system for hydrogen production, International Journal of Hydrogen Energy, https://doi.org/10.1016/j.ijhydene.2019.12.027

Overall system analysis

In this section, energy and mass balances of each component and the entire system are calculated using Aspen Plus simulation. Fig. 7 shows the flow diagram of the alkaline electrolysis plant with the results of the simulation at base case operation conditions (Table 2). Mass balances and enthalpies at specified conditions are shown, also heat losses and electrical consumption of different component are included. For easy understanding, the values of pressure and temperature of each stream are represented. The detailed composition of each matter flow is shown in Table 3.

From data obtained, it can be seen that when the system operates at current density of 0.42 A cm^{-2} (corresponding to a power required by the electrolysis process of 10 kW), it leads to a hydrogen production rate of 1.95 Nm^3 h^{-1} (0.17 kg h^{-1}, without taking into account the water in the stream) at 25 °C and 1 atm. As for the energy balance, the results show that the energy is perfectly balanced in the stack and the waste heat is indirectly retired in heat exchangers located in the electrolyte recirculation loops. The total excess heat is calculated to be 2392.8 W and it is dissipated by cooling water from an air-cooler system at 35 °C.

In order to analyse how the consumption of auxiliary components impacts on the efficiency system, the variation of net system power and stack power with current density at base-case conditions is presented in Fig. 8a.

It can be observed from Fig. 8a that, with the increase of current density the difference between the stack power and the net system power increases, which is due to the increase in parasitic loads. As a consequence, Fig. 8b shows that the consumption of the balance of the plant reduces the stack efficiency considerably and the reduction is higher when current density increases. At the specified operation point of 0.42 A cm^{-2}, stack efficiency is 57.9% and system efficiency is 53.3%. Also, in Fig. 8b can be seen that the efficiency initially increases at lower current densities reaching a peak and finally decreases with the increase of the current density. There is an operation point where system efficiency is maximized and the specific consumption reaches the minimum point. The maximum system efficiency obtained is 55.5% at a current density of 0.25 A/cm^2.

In Fig. 8c, the distribution of the electric power input is indicated at 0.42 A cm^{-2} and an analysis of the consumption of the auxiliary systems (pumps and fan) at the same point is shown in Fig. 8d, considering different temperatures and pressures. As it can be observed, the power required by the balance of the plant is less than 1 kW, increasing at lower temperature and higher pressure.

Finally, Fig. 9 shows the variation of the system efficiency with the temperature and pressure in an operating map at current density of 0.25 and 0.42 A cm^{-2} (corresponding to an electrolysis input power of 6 kW and 10 kW). As can be seen, when the temperature increases and the pressure diminishes,

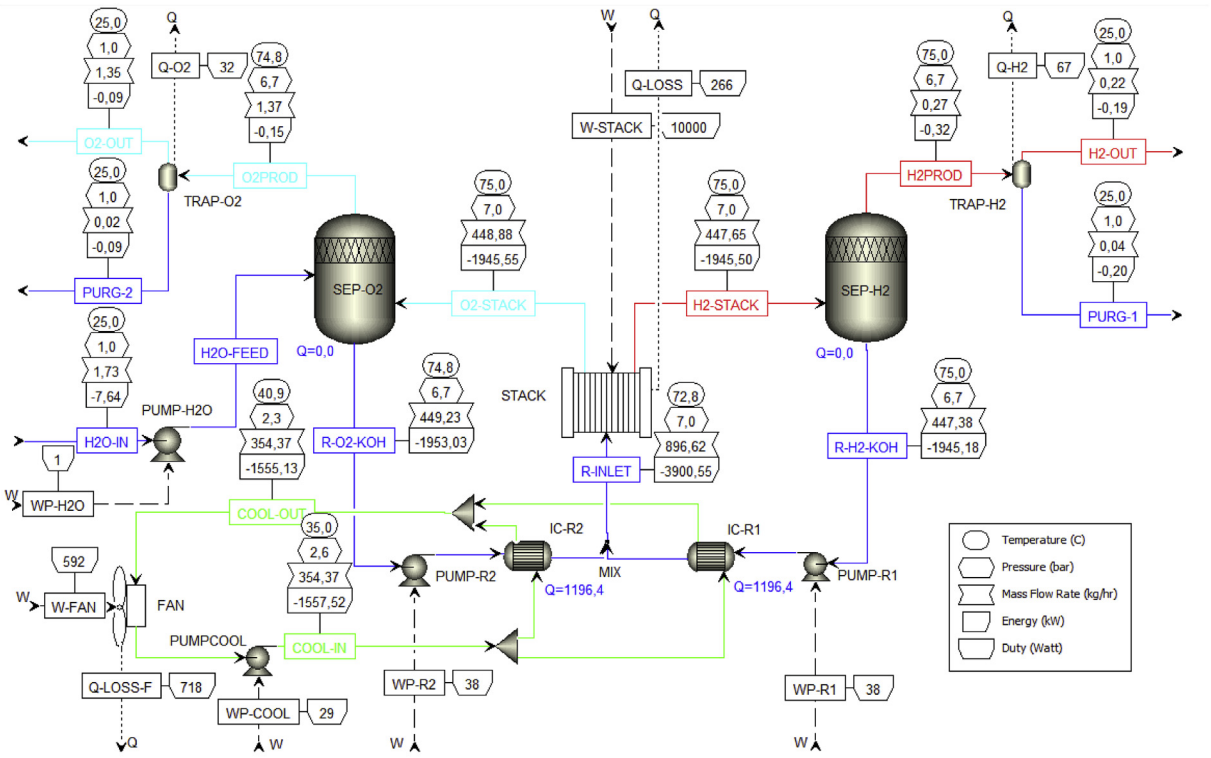

PUMP			SEPARATOR VESSEL			HEAT EXCHANGER			AIR COOLER					
Parameter	Value	Unit	Parameter	Value	Unit	Parameter	Value	Unit	Parameter	Value	Unit	Parameter	Value	Unit
Isentropic efficiency	70	%	Pressure drop	0.3	bar	Pressure drop	0.3	bar	Pressure drop	0.3	bar	Air pressure	800	Pa
Increased pressure	0.6	bar	Duty	Adiabatic		Efficiency	100	%	Motor efficiency	70	%	Air speed rotor	23	m/s

Fig. 7 – Energy and mass flow diagram of the system at base case operation conditions (10 kW, 75 °C and 7 bar).

Please cite this article as: Sánchez M et al., Aspen Plus model of an alkaline electrolysis system for hydrogen production, International Journal of Hydrogen Energy, https://doi.org/10.1016/j.ijhydene.2019.12.027

Table 3 – Composition of the matter flow at base-case operation conditions (75 °C and 7 bar).

Stream	T (°C)	P (bar)	Mass flow (kg h^{-1})	Composition (kg h^{-1})		
				H_2O	H_2	O_2
H2O-IN	25	1	1.730	1.730	0	0
H2O-FEED	25.49	7	1.730	1.730	0	0
H2-STACK	75	7	447.650	447.470	0.178	0
O2-STACK	75	7	448.870	447.470	0.000131	1.404
R–O2-KOH	74.81	6.7	449.230	449.150	0	0.07506
R–H2-KOH	74.99	6.7	447.380	447.370	0.00408	0
R-INLET	72.75	7	896.610	896.530	0.00409	0.07507
H2-PROD	74.99	6.7	0.260	0.095	0.173	0
H2-OUT	25	1	0.220	0.050	0.173	0
PURG-1	25	1	0.044	0.044	0	0
O2-PROD	74.81	6.7	1.374	0.045	0.000125	1.329
O2-OUT	25	1	1.353	0.024	0.000125	1.329
PURG-2	25	1	0.021	0.021	0	0

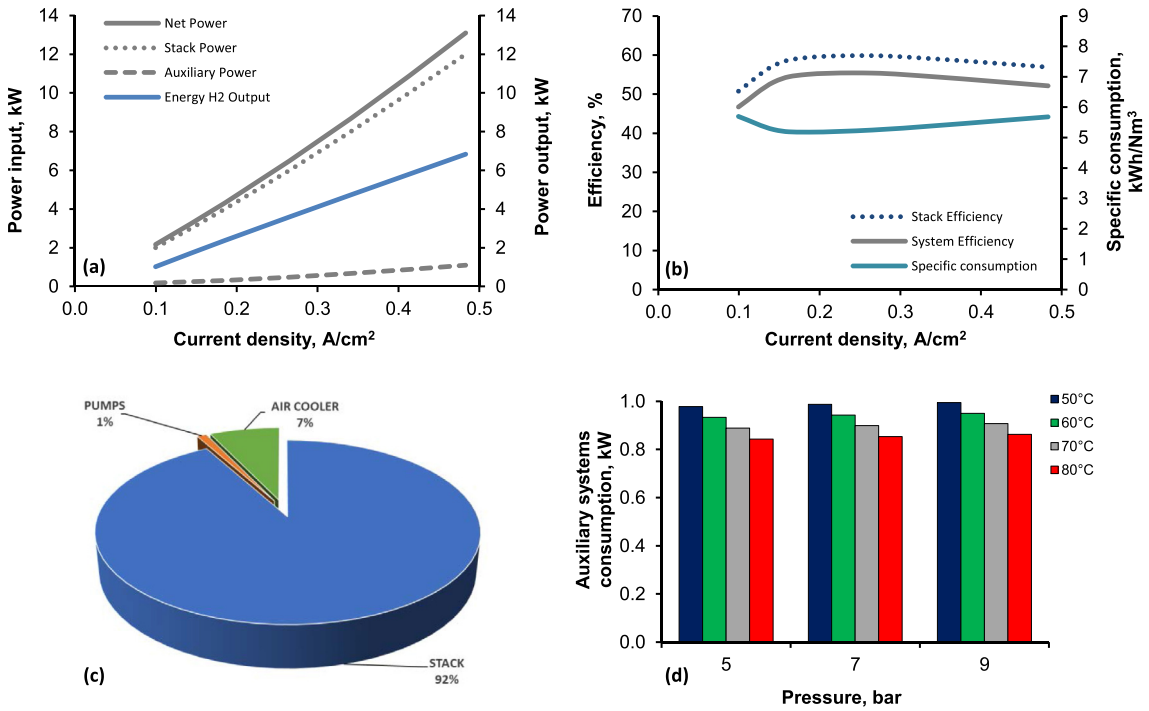

Fig. 8 – Energy system analysis at base-case conditions: (a) stack power, net power and auxiliary power; (b) stack and system energy efficiencies; (c) distribution of electric power input by components; (d) analysis of auxiliary system consumption: influence of the pressure and temperature.

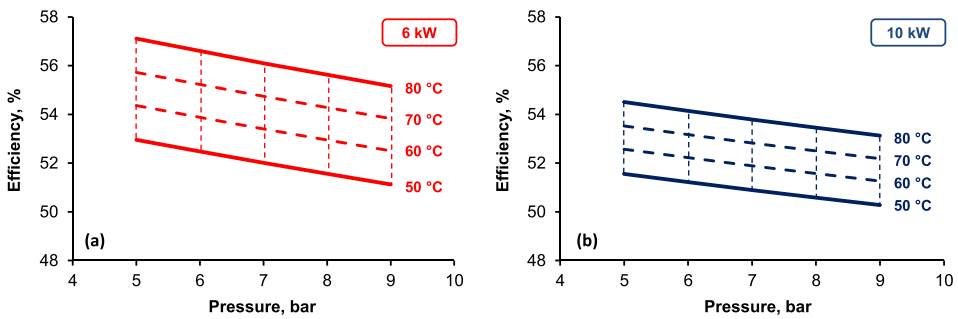

Fig. 9 – Operating map of the alkaline electrolysis system efficiency at an electrolysis input power of 6 kW and 10 kW.

Please cite this article as: Sánchez M et al., Aspen Plus model of an alkaline electrolysis system for hydrogen production, International Journal of Hydrogen Energy, https://doi.org/10.1016/j.ijhydene.2019.12.027

the overall efficiency improves. In this way, for example, if the operating temperature is 60 °C, a similar efficiency is obtained using 5 bar at 0.42 A cm^{-2} that 9 bar at 0.26 A cm^{-2}. On the other hand, when the pressure is 8 bar the efficiency is approximately the same at 75 °C and 0.42 A cm^{-2} than at 60 °C and 0.26 A cm^{-2}.

Therefore, the efficiency can be kept constant by decreasing the pressure if the current density is increased (always above operation point where system efficiency is maximized), or if the temperature and current density increase at the same time. So, this map establishes which parameter would have to be changed to reach a greater efficiency and it is a first indicator of process performance.

Conclusions

In this paper, an Aspen Plus model of an alkaline water electrolysis plant has been proposed with the objective of evaluating the performance of a complete system, including the stack and balance of plant, under different operating conditions, such as temperature and pressure.

For this purpose, a custom model of the electrolysis cells developed in a previous work has been integrated in Aspen Plus as a subroutine using Aspen Custom Modeler. This stack model is based on semi-empirical equations that describe the voltage cell, Faraday efficiency and gas purity as a function of the current density. The rest of the components in the electrolysis plant have been modelled with standard operation units included in Aspen Plus.

In order to ensure the accuracy and validity of the model, a comparison between the experimental data and the calculated values by the proposed model has been carried out. The RMS error is approximately 5 mV per cell and lower than 1% for the Faraday efficiency and HTO. So, the results show an excellent correlation, which demonstrates the usefulness of the model to predict the electrolyzer response in other experimental conditions.

On the basis of this, a parametric study has been conducted. It is observed that when the temperature increases from 50 °C to 80 °C, the voltage progressively reduces. As a consequence, the stack power required in the electrolysis decreases. On the other hand, an increase in the temperature leads to lower hydrogen rate due to that the Faraday efficiency is reduced and higher crossover of hydrogen to the oxygen side (HTO). With regard to the pressure, the stack voltage increases slightly when the pressure increases in the range studied (from 5 to 9 bar) and no variations are observed in hydrogen production. Also, the higher the pressure the higher the impurity of the gases produced.

In addition, the Aspen Plus model presented in this work enables to obtain mass and energy balances of each subcomponent and the entire system in a fast and accurate way. On the basis of this, it has been possible to analyse the thermodynamic system behaviour and identify the consumption of each component as well as energy losses sources. It has been observed that the power required by the balance of the plant is approximately 8% of the net power and reduces the stack efficiency up to 5%, being the reduction higher when current density increases. In particular, at reference conditions (7 bar and 75 °C) and current density of 0.42 A cm^{-2}, stack efficiency is approximately 58% and system efficiency is 53.3%.

Finally, an operating map has been used to quantify the most influential parameters in the overall system efficiency. It identifies which variable should be modified to achieve a greater efficiency. In general terms, the results indicate that the influence of the pressure is not as strong as the operation temperature in the investigated ranges. So, when the temperature increases and the pressure diminishes, the overall efficiency improves and the energy consumption is reduced. Particularly, for this alkaline electrolysis system the optimum operation conditions would be 5 bar and 80 °C reaching an overall system efficiency close to 58% at 0.25 A/cm^2.

In conclusion, the novel Aspen Plus proposed in this work provides a useful design tool that can be applied to maximize the efficiency and cost of an alkaline electrolysis system powered by renewable energy sources for hydrogen production. The obtained results allow determining which process variables are the most influential and hence, should be optimized in order to improve the performance and operation. This model can further be used in the future to develop a powerful tool to perform techno-economic analysis of alkaline electrolysis systems integrated with other process.

Acknowledgements

The work described in this paper has been developed in the facilities of the Centro Nacional del Hidrógeno (CNH2), whose financial supporters are Ministerio de Ciencia, Innovación y Universidades (MCIU, Spain), Junta de Comunidades de Castilla-La Mancha (JCCM, Spain) and European Regional Development Fund (ERDF).

REFERENCES

[1] Kotowicz J, Jurczyk M, Wecel D, Ogulewicz W. Analysis of hydrogen production in alkaline electrolyzers. J Power Technol 2016;96(3):149–56.
[2] Lehner M, Tichler R, Steinmüller H, Koppe M. Power-to-Gas: technology and business model. Cham (Switzerland): Springer; 2014.
[3] Buttler A, Spliethoff H. Current status of water electrolysis for energy storage, grid balancing and sector coupling via power-to-gas and power-to-liquid: a review. Renew Sustain Energy Rev 2018;82:2440–54.
[4] Bertuccioli L, Chan A, Hart D, Lehner F, Madden B, Standen E. Development of water electrolysis in the European Union. Cambridge (UK): FCH JU funded studies; 2014. Element Energy, Lausanne (CH); E4tech Sarl.
[5] Ursua A, Gandía LM, Sanchis P. Hydrogen production from water electrolysis: current status and future trends. Proc IEEE 2012;100(2):410–26.

Please cite this article as: Sánchez M et al., Aspen Plus model of an alkaline electrolysis system for hydrogen production, International Journal of Hydrogen Energy, https://doi.org/10.1016/j.ijhydene.2019.12.027

[6] Michal J, Daniel W, Zeng K, Zhang D. Recent progress in alkaline water electrolysis for hydrogen production and applications. Prog Energy Combust Sci 2010;36(3):307–26.
[7] Li X, Walsh FC, Pletcher D. Nickel based electrocatalysts for oxygen evolution in high current density alkaline water electrolysers. Phys Chem Chem Phys 2011;13:1162–7.
[8] Singh RN, Mishra D, Sinha ASK, Singh A. Novel electrocatalysts for generating oxygen from alkaline water electrolysis. Electrochem Commun 2007;9:1369–73.
[9] Pletcher D, Li X, Wang S. A comparision of cathodes for zero gap alkaline water electrolyzers for hydrogen production. Int J Hydrogen Energy 2012;37:7429–35.
[10] Li X, Pletcher D. Prospects for alkaline zero gap water electrolysers for hydrogen production. Int J Hydrogen Energy 2011;36:15089–104.
[11] Manabe A, Kashiwase M, Hashimoto T, Hayashida T, Kato A, Hirao K, Shimomura I, Nagashima I. Basic study of alkaline water electrolysis. Electrochim Acta 2013;100:249–56.
[12] Leng Y, Chen G, Mendoza AJ, Tighe TB, Hickner MA, Wang MA. Solid-state water electrolysis with an alkaline membrane. J Am Chem Soc 2012;134:9054–7.
[13] Xiao L, Zhang S, Pan J, Yang C, He M, Zhuang L, Lu J. First implementation of alkaline polymer electrolyte water electrolysis working only with pure water. Energy Environ Sci 2012;5:7869–71.
[14] Pavel CC, Cecconi F, Emiliani C, Santiccioli S, Scaffidi A, Catanorchi S, Comotti M. Highly efficient platinum group metal free based membrane-electrode assembly for anion exchange membrane water electrolysis. Angew Chem Int Ed 2014;53(5):378–81.
[15] Olivier P, Bourasseau C, Bouamama PB. Low-temperature electrolysis system modelling: a review. Renew Sustain Energy Rev 2017;78:280–300.
[16] Hammoudi M, Henao C, Agbossou K, Dubé Y, Doumbia ML. New multi-physics approach for modelling and design of alkaline electrolyzers. Int J Hydrogen Energy 2012;37:13895–913.
[17] Heano C, Agbossou K, Hammoudi M, Dubé Y, Cardenas A. Simulation tool based on a physics model and an electrical analogy for an alkaline electrolyser. J Power Sources 2014;250:58–67.
[18] Ulleberg Ø. Modeling of advanced alkaline electrolyzers: a system simulation approach. Int J Hydrogen Energy 2003;28(1):21–33.
[19] Hug W, Bussmann H, Brinner A. Intermittent operation and operation modeling of an alkaline electrolyzer. Int J Hydrogen Energy 1993;18(12):973–7.
[20] Busquet S, Hubert CE, Labbé J, Mayer D, Metkemeijer R. A new approach to empirical electrical modelling of a fuel cell, an electrolyser or a regenerative fuel cell. J Power Sources 2004;13:41–8.
[21] Vanhanen JP, Lund PD. Computational approaches for improving seasonal storage systems based on hydrogen technologies. Int J Hydrogen Energy 1995;20(7):575–85.
[22] Artuso P, Gammon R, Orecchini F, Watson SJ. Alkaline electrolysers: model and real data analysis. Int J Hydrogen Energy 2011;36(13):7956–62.
[23] Amores E, Rodríguez J, Carreras C. Influence of operation parameters in the modeling of alkaline water electrolyzers for hydrogen production. Int J Hydrogen Energy 2014;39(25):13063–78.
[24] Zhou T, Francois B. Modeling and control design of hydrogen production process for an active hydrogen/wind hybrid power system. Int J Hydrogen Energy 2009;3:21–30.
[25] Mori M, Mržljak T, Drobnič B, Sekavčnik M. Integral characteristics of hydrogen production in alkaline electrolysers. J Mech Eng 2013;59(10):585–94.
[26] Diéguez PM, Ursúa A, Sanchis P, Sopena C, Guelbenzu E, Gandía LM. Thermal performance of a commercial alkaline water electrolyzer: experimental study and mathematical modelling. Int J Hydrogen Energy 2008;33(24):7338–54.
[27] Zhang H, Su S, Lin G, Chen J. Configuration design and parametric optimum criteria of an alkaline water electrolyzer system for hydrogen production. Int J Electrochem Sci 2011;6:2566–80.
[28] Schmidt O, Gambhir A, Staffel I, Hawkes A, Nelson J, Few S. Future cost and performance of water electrolysis: an expert elicitation study. Int J Hydrogen Energy 2017;42:30470–92.
[29] Anderson T, Vijay P, Tade MO. An adaptable steady state Aspen Hysys model for methane fueled oxide fuel cell. Chem Eng Res Des 2014;92:295–307.
[30] Hauck M, Herrmann S, Spliethoff H. Simulation of a reversible SOFC with aspen Plus. Int J Hydrogen Energy 2017;43:10329–40.
[31] Rivera-Tinoco R, Farran M, Bouallou C, Auprete F, Valentin S, Millet P, Ngameri JR. Investigation of power-to-methanol processes coupling electrolytic hydrogen production and catalytic CO2 reduction. Int J Hydrogen Energy 2016;43:4546–59.
[32] JaeHwa K, DuckJoo Y, Chang HO. Simple electrolyzer model development for high-temperature electrolysis system analysis using solid oxide electrolysis cell. J Nucl Sci Technol 2010;47(7):590–607.
[33] Stoots CM, James EO, McKellar MG, Hawkes GL. Engineering process model for high-temperature electrolysis system performance evaluation. AIChe 2005 Annual meeting. Idaho National Laboratory; 2005.
[34] Sánchez M, Amores E, Rodríguez L, Clemente-Jul C. Semi-empirical model and experimental validation for the performance evaluation of a 15 kW alkaline water electrolyzer. Int J Hydrogen Energy 2018;43(45):20332–45.
[35] Hanyack ME. Chemical process simulation and the Aspen HYSYS v8.3. Software. CreateSpace Independent Publishing Platform; 2013.
[36] Dyment J, Mantrala V. Jump start: Aspen custom modeler v8.0. A brief tutorial. Aspen Technology, Inc.; 2015.
[37] Gandía LM, Arzamendi G, Diéguez PM. Renewable hydrogen technologies. Production, purification, storage, applications and safety. Amsterdam: Elsevier Publishing Company; 2013.
[38] Amores E, Rodríguez J, Oviedo J, de Lucas-Consuegra A. Development of an operation strategy for hydrogen production using solar PV energy based on fluid dynamic aspects. Open Eng 2017;7:141–52.
[39] Haug P, Koj M, Turek T. Influence of process conditions on gas purity in alkaline water electrolysis. Int J Hydrogen Energy 2017;42(15):9406–18.
[40] Ursua A, Marroyo L, Gubía E, Gandía LM, Diéguez PM, Sanchis P. Influence or the power supply on the energy efficiency of an alkaline water electrolyser. Int J Hydrogen Energy 2009;34:3221–33.
[41] Janssen H, Bringmann JC, Emonts B, Schroeder V. Safety-related studies on hydrogen production in high-pressure electrolysers. Int J Hydrogen Energy 2004;29:759–70.
[42] Ni M, Leung MKH, Leung DYC. Energy and exergy analysis of production by solid oxide steam electrolyzer plant. Int J Hydrogen Energy 2007;32:4648–60.
[43] Al-Ghandoor A, Phelan PE, Villalobos R, Jaber JO. Energy and exergy utilizations of the U.S. manufacturing sector. Energy 2010;35:3048–65.
[44] Sánchez M, Amores E, Rodríguez J, Sánchez-Molina M. Laboratorio de Electrólisis Alcalina del Centro Nacional del Hidrógeno: una instalación al servicio de la comunidad científico-tecnológica e industrial. In: Libro de Comunicaciones del Congreso Iberoamericano de Hidrógeno

Please cite this article as: Sánchez M et al., Aspen Plus model of an alkaline electrolysis system for hydrogen production, International Journal of Hydrogen Energy, https://doi.org/10.1016/j.ijhydene.2019.12.027

y Pilas de Combustible, Barcelona (Spain); October 15-17; 2014.
[45] Sánchez M, Hidalgo D, Quintana R, Saiz F. Influence of the design of liquid-gas separators in the operation of an alkaline water electrolysis system for hydrogen production: evaluation and optimization. In: 2nd ADEL International Workshop, Ajaccio (France); May 8–10; 2013.
[46] Sánchez M. Desarrollo de sistemas de producción de hidrógeno energético por generación alcalina: proyecto DESPHEGA. Revista Energética XXI 2013;136:26–7.
[47] Milewski J, Guandalini G, Campanari S. Modeling an alkaline electrolysis cell through reduced-order and loss estimate approaches. J Power Sources 2014;269:203–11.
[48] Tijani AS, Yusup NAB, Rahim AHA. Mathematical modelling and simulation analysis of advanced alkaline electrolyzer system for hydrogen production. Procedia Technology 2014;15:799–807.
[49] Ursúa A, Sanchis P. Static-dynamic modelling of the electrical behaviour of a commercial advanced alkaline water electrolyser. Int J Hydrogen Energy 2012;37:18598–614.
[50] Onda K, Kyakuno T, Hattori K, Ito K. Prediction of production power for high-pressure hydrogen by high-pressure water electrolysis. J Power Sources 2004;132:64–70.
[51] Mazloomi SK, Sulaiman N. Influencing factors of water electrolysis electrical efficiency. Renew Sustain Energy Rev 2012;16:4257–63.

Please cite this article as: Sánchez M et al., Aspen Plus model of an alkaline electrolysis system for hydrogen production, International Journal of Hydrogen Energy, https://doi.org/10.1016/j.ijhydene.2019.12.027